Electrochemical lossy mode resonance for detection of manganese ions

Ismel Dominguez [a], Jesus M. Corres [a,b,*], Ignacio Del Villar [a,b], Juan D. Mozo [c],
Radka Simerova [d], Petr Sezemsky [d], Vitezslav Stranak [d], Mateusz Śmietana [e], Ignacio R. Matias [a,b]

[a] *Electrical, Electronic and Communications Engineering Department, Public University of Navarra, 31006 Pamplona, Spain*
[b] *Institute of Smart Cities (ISC), Public University of Navarra, 31006 Pamplona, Spain*
[c] *Department of Chemical Engineering, Physical Chemistry and Materials Sciences. University of Huelva, 21071 Huelva, Spain*
[d] *University of South Bohemia, Faculty of Science, Institute of Physics and Biophysics, Branisovska 1760, 370 05 Ceske Budejovice, Czech Republic*
[e] *Warsaw University of Technology, Institute of Microelectronics and Optoelectronics, Koszykowa 75, 00-662 Warszawa, Poland*

ARTICLE INFO

ABSTRACT

In this work we propose electrochemical lossy mode resonance (eLMR) as a powerful method for the detection of manganese (Mn) ions. The sensor is based on a simple planar waveguide (soda—lime glass coverslip) coated with a thin layer of indium tin oxide (ITO) to obtain an optical resonance effect. Simultaneously, the ITO layer served as the working electrode in the cathodic stripping voltammetry (CSV) of Mn. The eLMR sensor is capable of simultaneously performing electrochemical (EC) and optical measurements, specifically lossy mode resonance (LMR), to monitor the growth of the adsorbed Mn layer on the ITO electrode and the electrochemically modulated diffusion layer. For Mn^{2+} ions, a limit of detection (LoD) of 1.26 ppb has been demonstrated using the EC method, whereas the optical method exhibited a LoD of 67.76 ppb. The results obtained indicate significant potential for application in molecular electrochemistry and studies focused on electrified interfaces.

1. Introduction

Manganese (Mn) plays an essential role in multiple biochemical reactions such as the metabolism of iron and proper operation of the brain. Like other metals present in the human body, when its concentration increases above a certain limit, it causes various dysfunctionalities such as neurotoxicity, male infertility, learning difficulties, memory loss and also development of the psychiatric neurological disorder known as manganism [1]. The European Environment Agency has set a limit of 50 µg/L (50 ppb) for Mn in drinking water [2].

A variety of detection methods are used for the determination of Mn concentration. The most common analytical procedures for measuring Mn levels in biological and environmental samples are atomic absorption spectroscopy (AAS) and atomic emission spectroscopy (AES) [3]. Other methods applied include inductively coupled plasma—mass spectrometry (ICP-MS) [4], spectrophotometry [5], neutron activation analysis [6], and x-ray fluorimetry [7]. Additionally, electrochemical (EC) techniques are widely used and they offer a number of benefits, i.e., they are inexpensive, portable, and easy to miniaturize [8]. Among the EC techniques [9], stripping voltammetry has a proven ability to analyze traces of metal ions [9]. Its low limit of detection is originated by the

predeposition stage used to accumulate the analyte on the electrode surface. Cathodic stripping voltammetry (CSV) is the most widely used EC technique for the determination of Mn [9]. Mn^{2+} is deposited on the surface as MnO_2 following the reaction given in (1) by applying the proper fixed potential and then redissolved with a voltammetric cathodic sweep of potentials.

$$Mn^{2+}(H_2O)_x(aq) \leftrightarrow MnO_2(H_2O)_{x-y}(s) + 4H^+ + (y-2)H_2O + 2e^- \tag{1}$$
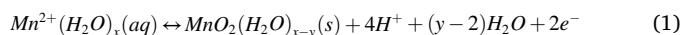
Various materials can be used as working electrodes for Mn detection. These include glassy carbon, boron-doped diamond, carbon nanotubes, palladium and platinum [10–14]. Among optically transparent electrode (OTE) materials, indium tin oxide (ITO) has been widely applied in spectroelectrochemical (SEC) sensing, where the optical properties of analytes are measured simultaneously with the EC response [15–20]. The wide positive potential window of ITO, reaching from − 1–1.75 V against Ag/AgCl 0.1 M KCl, makes it a very useful compared to other material for the electrodes, such as gold [21]. Recently, ITO has been used in the CSV technique for Mn^{2+} detection in water samples [22] and whole blood [23].

In addition, due to its unique optical properties, ITO has also been widely used in optical sensing, including the sensors relying on lossy
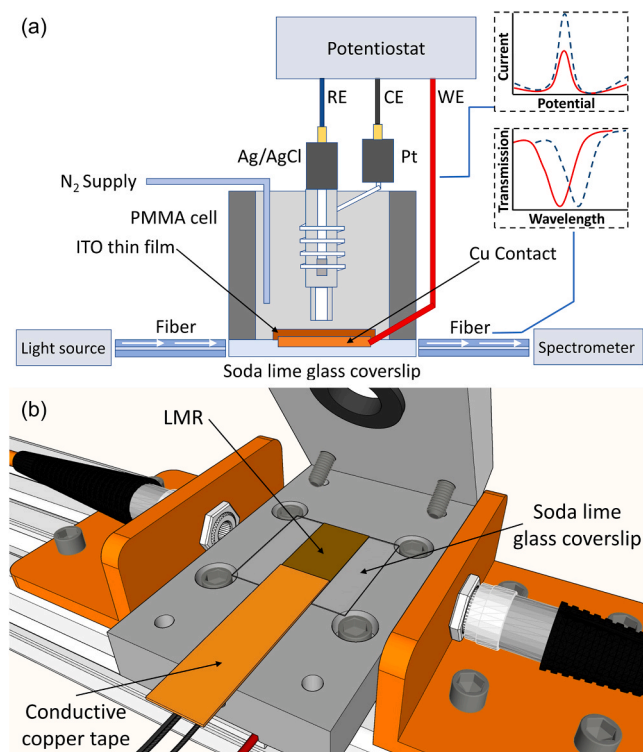

Fig. 1. Experimental setup used for sensor monitoring: (a) schematic representation of the experimental setup cell arrangement including coverslip coated with ITO thin film as a working electrode (WE), reference electrode (RE) and counter electrode (CE); (b) the coverslip arrangement in the setup supported by a broadband light source, spectrometer and potentiostat.

mode resonance (LMR), achieved on both optical fibers and planar substrates [24]. When the LMR is generated, light guided in the waveguide or optical fiber core is attenuated due to the mode coupling to the thin film [25]. The central wavelength of the resonance, i.e., the wavelength range of operation, can be tuned by adjusting the thickness and optical properties of the film [26].

LMR sensors are capable of real-time monitoring of changes in the optical properties, specifically the refractive index (RI), of thin film surfaces resulting from affinity interactions between the LMR-generating thin film and ions or molecules in a solution. One interesting aspect of LMR-based sensors is that they can be cost-effective to fabricate and are suitable for miniaturization. However, detecting small molecules using the conventional LMR approach can be challenging because small differences in the refractive index require high sensor sensitivity and stability. Nevertheless, this limitation can be easily overcome by combining EC measurement with the LMR response (eLMR) in the same sensing device, especially when the analyte is redox-active and common voltammetric techniques are employed [27].

In an eLMR setup, the thin layer is functional in dual domains, i.e., generating LMR and as the working electrode of the standard three-electrode EC setup. In this approach, in addition to the optical properties, also the thickness of the LMR generating film has to be optimized [28]. Since the thin film resistance is inversely proportional to the thin film thickness, it needs to be high enough to obtain the EC response. However, the sensitivity of the high-order LMR observed for thicker layers is lower than that for the low-order resonances achieved for thin films. Therefore, the thickness and other properties of the film must be chosen taking into account both factors.

There has been study of the dependences between the EC potential and the LMR shift caused by changes in RI of both ITO and the surrounding solution during the electrode potential modulation [29]. The simultaneous application of optical and EC techniques provides

enhanced information about the analyte and its interaction with the electrode and makes it possible to identify species contributing to intermediate or final products of the reactions [30]. In a recent work, the application of optical fiber sensors based on LMR for the monitoring of EC processes has been discussed [31]. The ITO-coated fiber-based device was used as the working electrode in a cyclic voltammetry (CV) EC setup to analyze the performance of redox reactions of ferrocyanides. The same principle has also been reported for the detection of two electro-active species (ferrocyanide and methylene blue), being able to reach limits of detection of 7.5 and 25.3 μM, respectively [32]. Moreover, it has been shown that in this configuration it is possible to perform a dual-domain label-free biosensing enhancement of performance by electrodeposition of PEDOT:PSS or detection of ketoprofen during its electropolymerization [27,33–35]. However, optical-fiber-based sensors, due to their tiny size, offer a limited active surface area.

In this work a classical EC configuration has been adapted to planar waveguide supporting LMRs. Using the proposed arrangement, the redox reaction of potassium ferrocyanide $K_3[Fe(CN)_6]$ (LMR and CV analysis) and the detection of Mn ions (LMR and CSV analysis) have been observed.

2. Materials and methods

2.1. Chemicals and materials

A 1000 μg/mL Mn^{2+} in 5% of HNO_3 atomic absorption standard was purchased from Alfa Aesar and diluted to obtain the desired concentrations. Ultrapure water (18.1 MΩ/cm) was obtained from a Barnstead Inc. water purification system and used to prepare all the standard solutions used. Glacial acetic acid (99.7%, Sigma-Aldrich) and sodium acetate (Fisher Scientific) were mixed in different proportions to yield a pH 5.0 acetate buffer used for analyses. Potassium nitrate (99.0%) was purchased from Sigma-Aldrich.

The electrically conductive and optically transparent ITO films were deposited on 160 μm thick soda—lime coverslips for microscope glass slides using magnetron sputtering of the ITO target (In_2O_3-SnO_2- 90/ 10 wt% and purity of 99.99%). The magnetron was driven by the RF power source COMET Cito1310 (13.56 MHz, 300 W). The deposition experiments were carried out at pressure p = 0.1 Pa in Ar atmosphere. The details of the deposition procedure can be found in [36]. Additionally, the coverslip surface was partially masked using Kapton tape.

2.2. Instrumentation

The film resistance of the working electrode was measured with a T2001A3 4-point probe device by Ossila. CV and CSV measurements were performed in a 10 mL conventional three-electrode system with a PMMA cell containing ITO-coated coverslips (50 Ω/sq, 100 nm thin film) with 7 mm × 18 mm area as a working electrode, an Ag/AgCl reference electrode (3.0 M KCl solution), and a platinum (Pt) coil wire (a diameter of 0.5 mm and 10 coils of 8 mm in diameter) as a counter electrode. The reference and counter electrodes were purchased from Redox.me. A copper tape was used to connect the ITO film to the potentiostat (Metrohm μSTAT200). Plastic cladding fibers of 230 μm were used to couple the light to the substrate. A Takhy HP wide spectrum source and Nirquest spectrometer from Ocean Optics were used to monitor the LMR. A gaseous nitrogen facility was also included to deoxygenate the solution under study and to mix it when the analyte was added. Additionally, the temperature of the working electrode was regulated to better control the reactions. Fig. 1 shows a detailed scheme of the cell.

Before the experiments, the PMMA cell container and counter electrode were sonicated twice for a period of 10 min in ultrapure water. The reference electrode was also washed with ultrapure water and isopropanol. All materials were dried in nitrogen. Different ITO-LMR samples were used for measurements in $K_3[Fe(CN)_6]$ and for Mn^{2+}
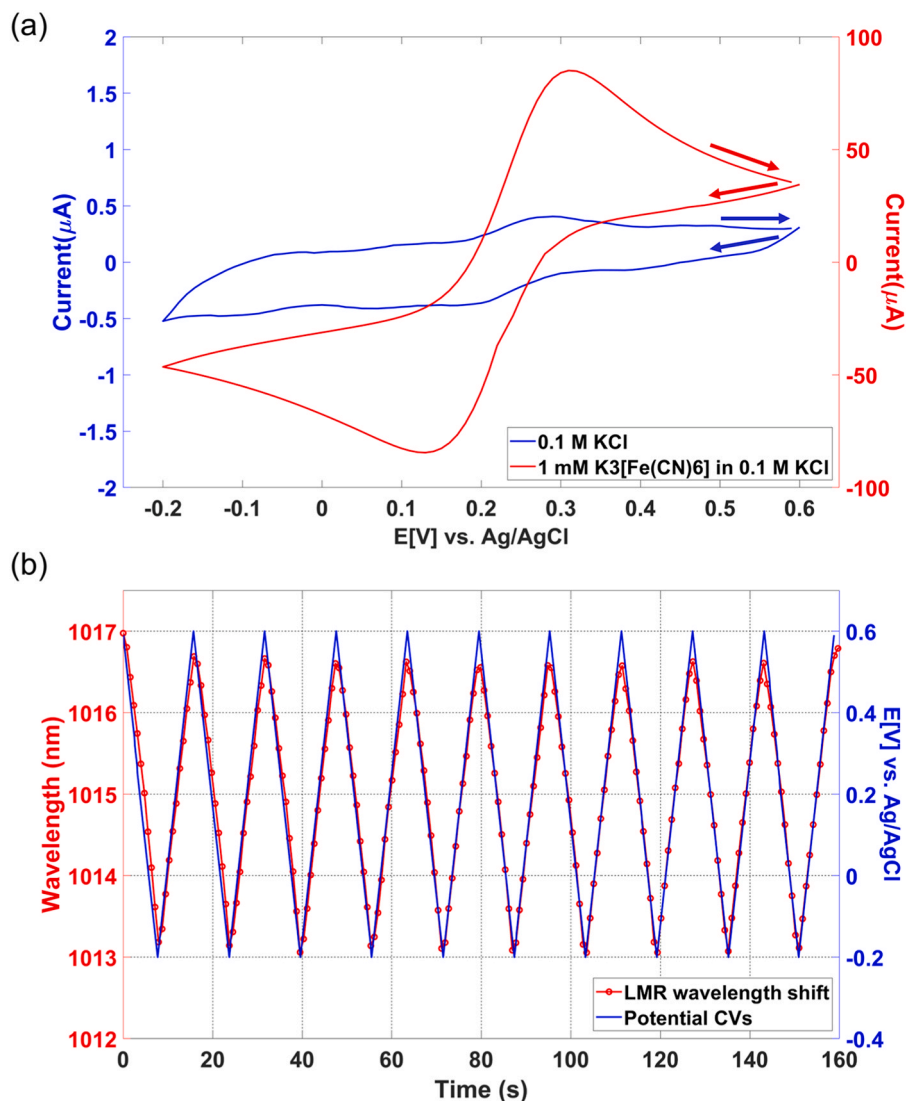
Fig. 2. (a) CV response of the sensor obtained in KCl 0.1 M and the redox probe of 1 mM $K_3[Fe(CN)_6]$ in 0.1 M KCl at 100 mVs^{-1} scan rate; (b) LMR wavelength shift in the transmission spectrum during 10 consecutive CV scans.

detection.

2.3. Modulation of ITO optical properties

As explained in [29], crystalline ITO can be obtained at low pressure (below 0.2 Pa). In such conditions, the resistivity of the material can be low and this makes it possible to achieve higher redox current peaks. However, as the pressure is reduced, the optical response due to the optical properties of the film is reduced (lower visibility and sensitivity of the LMRs). Therefore, depositing at very low pressures is not recommended and a compromise value of 0.1 Pa is adopted, which demonstrated good performance in both the EC and optical domains.

3. Results

3.1. EC properties of ITO thin film

The performance of the ITO electrode was evaluated as a working electrode with the classical redox reactions of $K_3[Fe(CN)_6]$ using the CV method [31]. A redox probe solution containing 1 mM $K_3[Fe(CN)_6]$ in 0.1 M KCl was prepared. In this experiment, the CV was applied at a scan rate of 100 mV/s in the range of 600 mV to − 200 mV. Fig. 2(a) shows

the comparison between the EC readouts in a 0.1 M KCl buffer solution and the one containing the redox probe. No additional peaks indicating contamination of the ITO electrode were observed.

Next, ten CV cycles were performed to check the stability of the ITO electrode and the reversibility of the EC redox reaction. The redox current peak separation reaches $\Delta E = 180$ mV, and it is similar to the value obtained for ITO deposited on optical fibers in the previous experiments [31]. It must also be noted that the redox reactions are highly reversible.

Fig. 2(b) shows the shift of the LMR wavelength during the CV cycles. The shift of the resonance is mainly due to the optical modulation of the LMR induced by the applied potential and its effect on the electrode—solution interface. A more detailed LMR wavelength shift versus potential versus current sensorgram is shown in Fig. S1 in the Supplementary Material.

Two parameters can be used to quantitatively analyze the LMR response [31]: the LMR wavelength shift and the transmitted power at a specific wavelength [27] (1060 nm in this work). Fig. 3(a) shows the evolution of both these parameters throughout the ten CV cycles, while Fig. 3(b) shows the spectral evolution of the LMR during the latter cycle. The two parameters analyzed have a direct linear response with the potential sweep. The linear response observed for this ITO electrode and
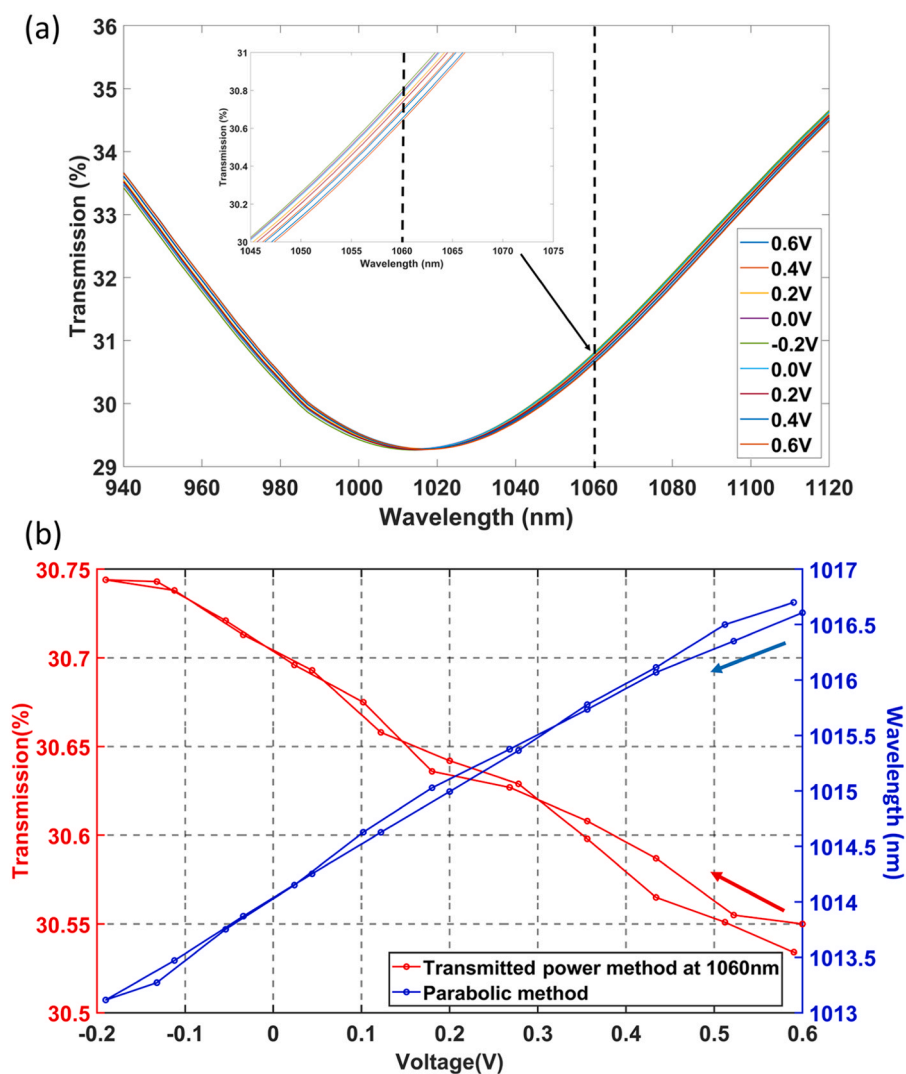
Fig. 3. Optical response of the LMR sensor to CV between 0.6 and − 0.2 V with a scan rate of 100 mV/s in 0.1 M KCl solution containing $K_3[Fe(CN)_6]$ 1 mM: (a) Spectral evolution of the LMR for the 10th CV cycle; (b) Shift of the LMR wavelength and variation of the lateral slope of the LMR at the specific wavelength of 1060 nm for the 10th CV cycle.

the redox reactions of $K_3[Fe(CN)_6]$ verify that the electrode is stable, which is essential for its further EC performance.

3.2. Detection of Mn^{2+} with eLMR sensor

Next, the CSV technique was applied to detect Mn ions using the eLMR system. Different concentrations of Mn^{2+} were prepared in 0.2 M buffer acetate (pH 5.0) in a 5% HNO_3 solution. The solution was stirred and deoxygenated (N_2 bubbling for 1 min).

According to [22], in order to oxidize the Mn^{2+} and create a MnO_2 layer on the ITO film, it is enough to apply a potential of 1200 mV and sweep it in the negative direction in order to be able to measure the current produced by the detachment of the MnO_2. Thus, a predeposition time was set to 10 min at a potential equal to 1200 mV. Overall, three CSV cycles per concentration were run between 1200 mV and 0 mV at a scan rate of 100 mV/s.

Fig. 4(a) shows the last CSV response out of three for each concentration. A well-defined response to Mn^{2+} at concentrations as low as 50 ppb has been obtained. The reduction peak of MnO_2 can be observed at a potential of 570 mV. Fig. 4(b) shows a sensorgram for the corresponding LMR wavelength shift. In addition to the LMR shift due to the predeposition, during the course of the experiment there is no return of the LMR peak to its origin. This is due to the cumulative effect of the

adsorption of MnO_2 to the area of the ITO electrode, an effect that is different from that observed for the CV analysis, where only the charge transfer is detected. It must be noted that the LMR wavelength is related to the thickness of the layer adhered to the ITO electrode.

In order to understand the observed process better, the first of the three cycles of 300 ppb is shown in Fig. 5. When the predeposition starts, there is a progressive LMR wavelength shift, which is due to the deposition of MnO_2 on the ITO electrode surface. After the predeposition, a stripping step is performed to complete the CSV cycle. This is done by progressively reducing the potential to 0 V, which leads to the recovery of the initial LMR wavelength, and again sweeping the potential up to 1200 mV with the same sweep rate and finally leaving a potential floating (the LMR wavelength shifts slowly to lower wavelengths). The LMR moves from an initial position of 1011.5–1015 nm when the predeposition begins, which consists of 10 min at a potential equal to 1200 mV. The complete evolution along the 21 cycles can be found in Fig. S2 in the Supplementary Material.

Additionally, the possibility of regeneration of the sensors used has been verified. To demonstrate this, at the end of the experiment with Mn^{2+}, the sensor was applied a potential of 0 V for 15 min, which allowed the redissolution of Mn^{2+} in the buffer, as shown in Fig. 4(b). This in turn caused the LMR wavelength to return to its initial value, indicating the absence of oxidized Mn^{2+} on the ITO surface. However, in
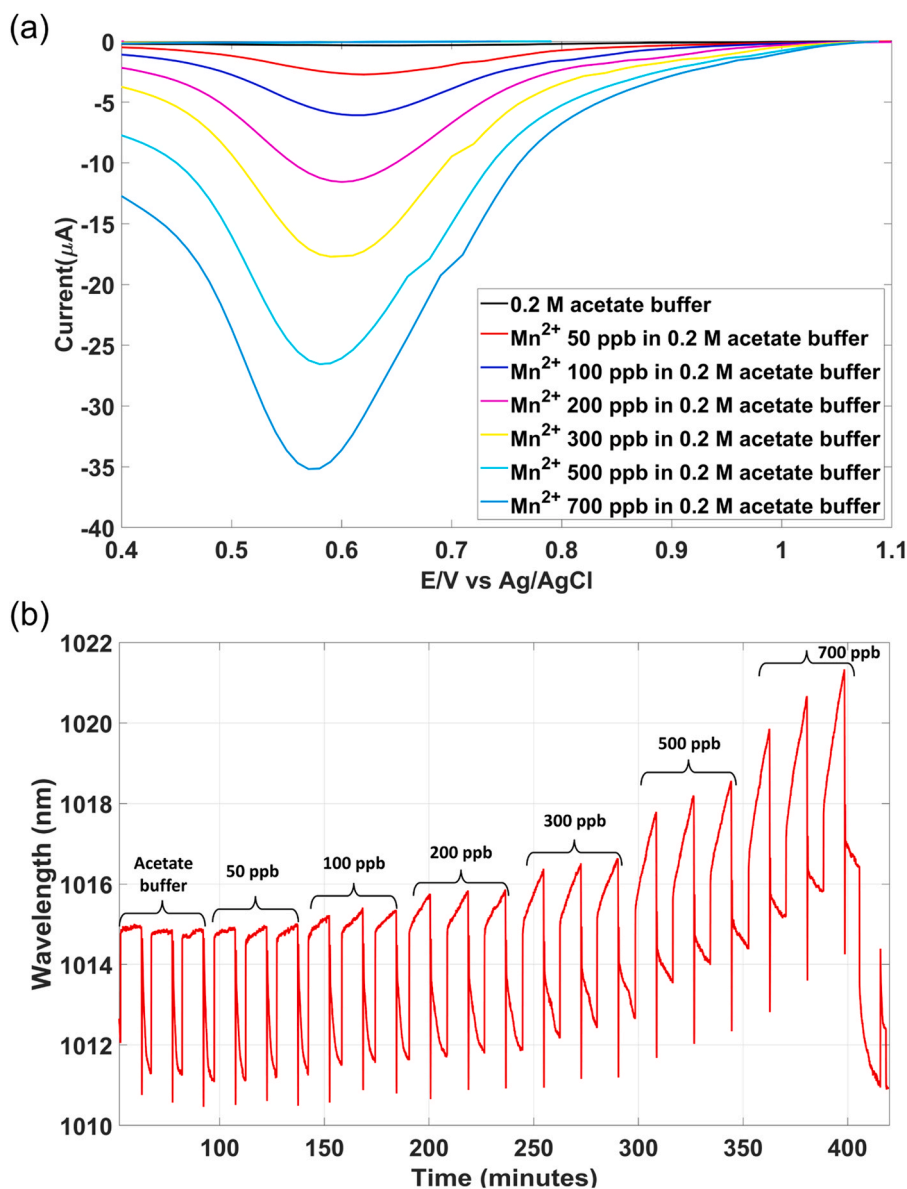
Fig. 4. Voltammograms of cathodic extraction within increasing concentrations of Mn^{2+}: (a) CSV in pH= 5.0 acetate buffer (last cycle out of three cycles at each concentration); (b) Sensorgram for the LMR response. Predeposition potential was set to 1200 mV and for 10 min.

order to investigate this process in detail, it is necessary to modify the cell by transforming it into an EC flow cell, which would allow for extracting the buffer with the dissolved analyte while the redissolution potential (0 V) is active and repeating the CSV cycles. Additionally, another option could be to apply linear sweep-cathodic stripping voltammetry (LS-CSV) instead of CSV, which would guarantee the gradual recovery of the sensor throughout the sensorgram, a strategy that will be taken into account in future experiments.

3.3. Visualization of the EC phenomenon in the LMR

The stripping process presented in Fig. 5 will be analyzed here in detail. Fig. 6 shows the optical monitoring of the MnO_2 reduction process in a new experiment carried out in similar conditions (the complete experiment is shown in Fig. S5 in the Supplementary Material), changing only the scan rate of the voltammetry in order to obtain a sufficient number of samples to observe the phenomenon [29]. Fig. 6(a) shows the optical response of the LMR compared to a straight line representing the linear change due to modulation, while Fig. 6(b) shows the potential and

current responses. Fig. 6(c) shows the result of subtracting the modulation effect from the optical response shown in Fig. 6(a). This makes it possible to increase the visibility of the perturbation in the optical response due to the MnO_2 reduction stage. The moment when this occurs agrees well with the current response shown in Fig. 6(b), which suggests that it is possible to correlate the optical response with the redox potential of the analyte. The complete evolution along the 9 cycles (200, 300 and 500 ppb) can be found in Fig. S5 in the Supplementary Material.

3.4. Analytical performance of the eLMR

Two working electrodes were used to calculate the LoD for Mn^{2+}. Fig. 7 shows the optical and EC calibration curves of three experiments, two of them performed with the same sensor. The graphs show the lineal fitting curve of the experimental points. The optical calibration curve was obtained with the average value of three slopes of the wavelength shift obtained for each of the three cycles of CSV, whereas the EC calibration curve was calculated with the average value of the three current values obtained for each of the three cycles of CSV.
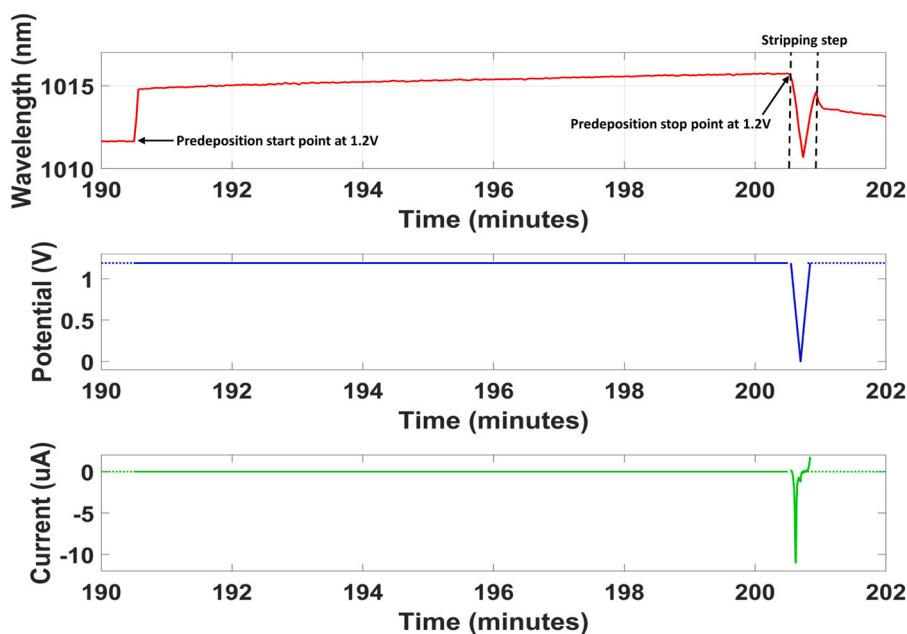
Fig. 5. Zoomed evolution of LMR wavelength, potential and current for 13th CSV cycle at 300 ppb of Mn^{2+}.
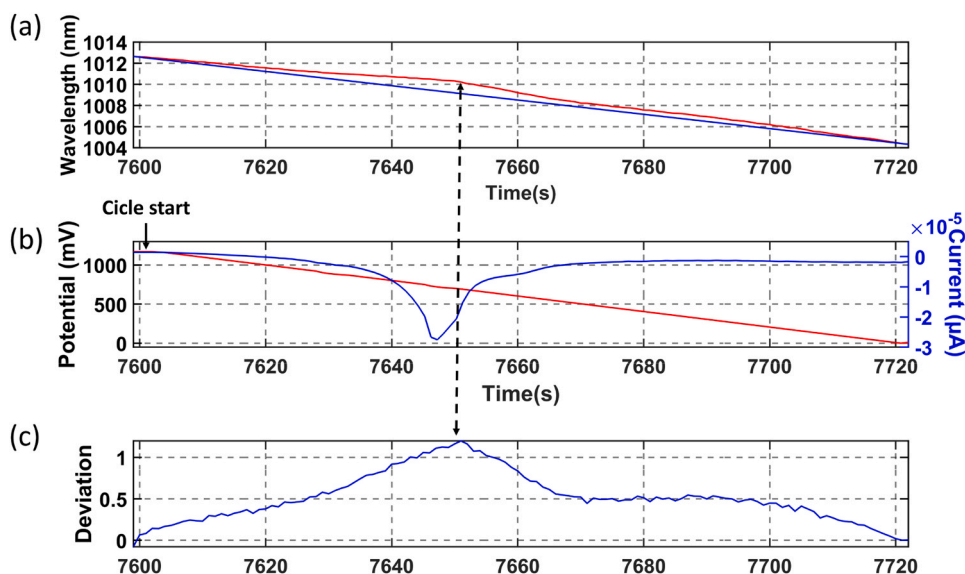

Fig. 6. EC and optical responses after predeposition with an increased resolution: (a) LMR wavelength with a straight line representing the modulation; (b) Potential and the current responses; (c) Result of subtracting the LMR and the straight line connecting its maximum with the minimum.

It is possible to observe a variation after the injection of as little as 50 ppb of Mn^{2+} with both the optical and EC techniques The LoD in the optical and EC domain is 67.76 ppb and 1.26 ppb, respectively, when calculated as three times the standard deviation at lower concentration divided by the slope. The EC and optical response repetition for sensor 1 can be observed in Fig. S3(a)-(b) in the Supplementary Material and a third experiment for sensor 2 can be observed there in Fig. S4(a)-(b).

The LoD calculated for the sensors used of 1.26 ppb (21 nM) for the detection of Mn^{2+} is an expected value for a CSV-type technique. Compared with other similar electroanalytical techniques [9], there are more efficient techniques than CSV, such as differential pulse sputtering voltammetry (DP-CSV) or square wave cathodic stripping voltammetry (SW-CSV). Moreover, there is a great variety of working electrodes to be used, deposition times, and actual samples. Depending on these, the LoD stays in the range of 0.01–740 nM. The sensors used in this research with

a LoD of 21 nM could be positioned in a medium range. The LoD for the methods approved by the Agency for Toxic Substances and Disease Registry of the US Department of Health and Human Services for quantifying manganese (such as AAS, ICP-AES, ICP-MS, and others) is mentioned in table 7.2 of [3], where this parameter ranges from 0.002 ppb to 10 ppb. By comparison, our method, with a LoD of 1.26 ppb, surpasses some of the methods proposed in [3], thereby reaffirming its position within the mid-range.

According to the LoD, the sensitivity of the sensor, the linear range of response, and relative standard deviation (RSD) values provided in Table 1, it can be observed that the electrochemical method exhibits 12 times higher sensitivity for detecting Mn^{2+} compared to the LMR sensor. Similarly, the RSD highlights the EC sensor as the best sensor, which is also verified by comparing the LoD of both methods. The analysis of minerals in drinking water and mineral water samples with RSDs lower
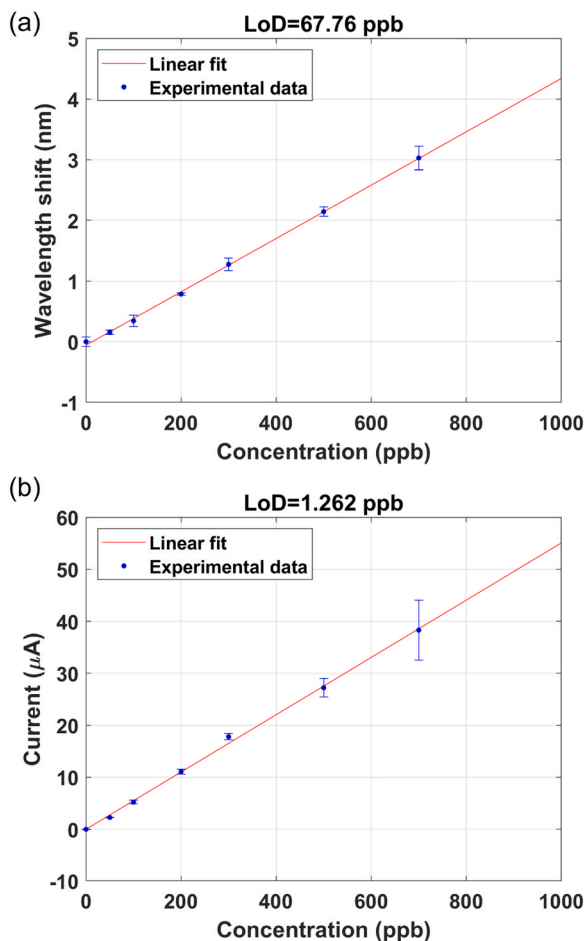
(a)

(b)

Fig. 7. Calibration curve of three experiments (n = 3) for detection of Mn^{2+} ions in buffer obtained with the lineal fitting curve of the experimental points for the: (a) average value of the three slopes of the LMR wavelength shift obtained for each of the three cycles of CSV; (b) average value of the three current values obtained for each of the three cycles of CSV.

Table 1
Analytical performance of the both methods eLMR offer, EC and optical.

Method	LoD (ppb)	Sensitivity	Linear range (ppb)	RSD (%)
EC	1.262	55.1 nA/ppb	50 – 700	6.34
LMR	67.76	4.40 pm/ppb	50 – 700	18.80

than 8% is considered accurate [37,38], which indicates that this method could be used to quantify Mn^{2+} in these kinds of water. On the other hand, in order to decrease the RSD of the LMR sensor (18.8%), its sensitivity must be improved.

3.5. Selectivity of the eLMR

In order to demonstrate how selective ITO can be with Mn, the experiments were repeated with the same ITO electrode using Mn^{2+}, Cu^{2+} and Fe^{2+} ions separately in similar concentrations. The selection of these metals is due to the fact that in some of the reviewed references they are analytes that can interfere with the detection of Mn^{2+} since their redox potential is close, so they can be easily oxidized in the ITO electrode. Fig. 8 shows that, for similar concentrations of analyte, the shift of the LMR is different for each type of ion, with Mn^{2+} showing the greatest wavelength shifts, up to nine times greater than for Cu^{2+}. Although the results obtained show that there is an affinity between ITO and Mn, this can be improved by preparing the surface of the working electrode with

materials capable of oxidizing only Mn [22].

The current sensorgram of these experiments is also shown in Fig. 9, where it can be seen once again that the ITO electrode is more sensitive to the detection of Mn^{2+} than to the rest of the ions.

Based on the cross-sensitivity results, the sensor used for detecting Mn^{2+}, Cu^{2+} and Fe^{2+} ions exhibits sensitivities of 8.56 pm/ppb, 2.29 pm/ppb and 1.63 pm/ppb, respectively. Considering the European regulation limits for drinking water, which are 50 ppb for Mn^{2+}, 2000 ppb for Cu^{2+}, and 200 ppb for Fe^{2+}, the displacement values for the eLMR sensor can be calculated. For Mn^{2+}, the sensor displaces 0.75 nm, for Cu^{2+} it displaces 4.5 nm, and for Fe^{2+} it displaces 0.24 nm. Based on these findings, it can be deduced that Fe^{2+} ions do not pose a problem for the detection of Mn^{2+} since the displacement is relatively small. However, for the recommended concentrations of Cu^{2+}, the detection of Mn^{2+} would be nullified due to the significant displacement. To overcome this issue, the sensor could be made specific to Mn^{2+} ions by utilizing the SSEBS polymer, as in [22]. The series of experiments carried out over 1 year showed stability throughout the period. In these tests, the response time of the sensor was configured for about 10 min, which was the predeposition time chosen to obtain a lower LoD, taking advantage of the CSV technique.

4. Discussion and conclusions

This work has verified the capability of a new electrochemical lossy mode resonance (eLMR) platform in planar substrate configuration towards biological and environmental applications. For this purpose, the detection of Mn^{2+} in water has been assessed.

The technically simple eLMR platform combines two important domains, EC and optical, for detection purposes. First, this new configuration was tested with $K_3[Fe(CN)_6]$, where a linear response was offered by the ITO electrode that verifies that the ITO electrode is stable.

Second, it was found experimentally that with both optical and EC analysis it is possible to detect Mn^{2+} ions. The current peaks of the EC process make it possible to measure the Mn^{2+} concentrations and calculate a detection limit of 1.26 ppb. At the same time, the optical monitoring of the LMR makes it possible to observe the cumulative effect of Mn adhered to the ITO electrode. This information can be used for design strategies directed to the regeneration and reusability of the eLMR sensors. The limit of detection achieved observing the LMR wavelength shift during the predeposition stage was 67.76 ppb. However, this limit can be improved by using low refractive index waveguides that can increase substantially the RI sensitivity of the eLMR sensors. Through this strategy, it is possible to obtain devices that are extremely sensitive to RI changes in proximity to that of the water index, as demonstrated in [39]. Other strategies are the use of signal processing, light sources, detectors and the utilization of thin films that permit the generation of LMRs with higher sensitivity and low bandwidth, thus enhancing the figure of merit.

The results obtained indicate significant potential for application in molecular electrochemistry and studies focused on electrified interfaces. The ability to detect and differentiate the contributions in EC and optical readouts of the composition and structure of the interface is crucial to conduct detailed investigations in this field. Traditional approaches based on surface tension measurements using mercury drop electrodes are no longer used in practice, so these studies have been practically abandoned due to the lack of availability of techniques offering sufficient sensitivity. LMR as a technique complementary to EC ones can be considered as an alternative, since it is capable of the detection of molecular-level changes on solid surfaces.

The eLMR platform can also be applied to the identification of heavy metal ions other than Mn^{2+}. Here, it has been observed, during the stripping step after the predeposition stage, that there is a divergence of responses compared to the modulation due to the linear variation of the potential. This divergence fits with the moment when the current response experiences a maximum variation, which is used for
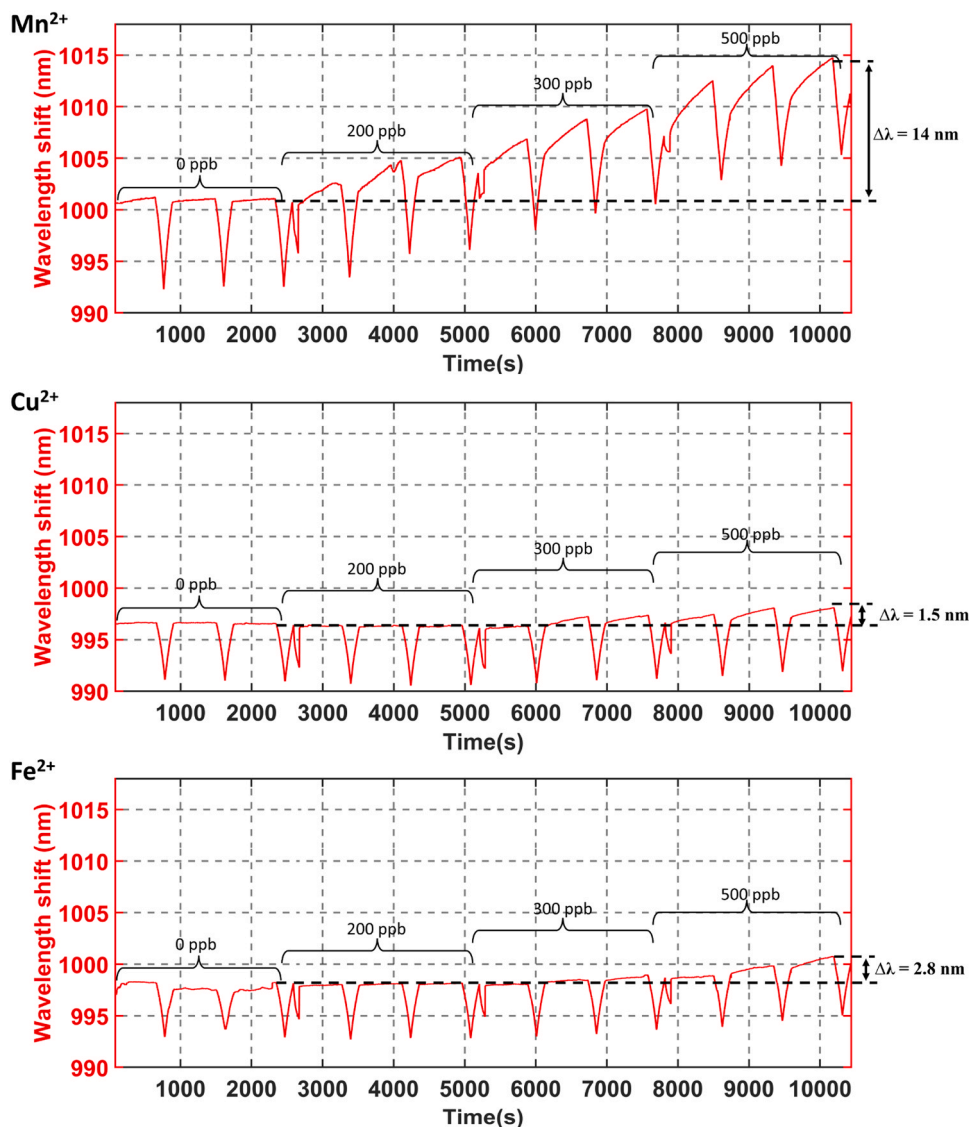
Fig. 8. Sensorgrams of the selectivity experiments carried out with Mn^{2+}, Fe^{2+} and Cu^{2+} ions.

identifying the redox potential of the material. This could be used to detect materials and increases the potential of the optical detection part.

Related to this, a path to follow in future research is to enhance the discriminated detection of specific analytes; especially heavy metals such as lead, copper, and cadmium could be developed. On the other hand, LMR is a quite versatile method that permits multiparameter detection [40], which suggests that multiparameter sensing with a single SEC platform could be achieved. In addition, this planar configuration could be used in the near future to integrate all the necessary electrodes in the same device, reaching a higher level of integration and repeatability than the proposal shown.

Thus, the eLMR method can become a versatile analytical tool, to detect not only metal ions, but also biomarkers, RNA, virus and other small chemical species. In addition, the in situ electrosynthesis of thin conducting polymers (such as PABA, PAP, among others) as support for covalent immobilization of antibodies can be a straightforward approach to build the sensing platforms taking advantage of eLMR monitoring for easy optimization of polymer thickness. In summary, there is a great potential in the proposed structure, which could reach the commercialization level for environmental, food quality and medical diagnosis applications.

CRediT authorship contribution statement

Ismel Dominguez: Methodology, Investigation, Writing, **Jesus M. Corres:** Conceptualization, Methodology, Supervision, Writing - Review & Editing, **Ignacio Del Villar**: Writing - Review & Editing, Formal analysis, **Juan D. Mozo**: Writing - Review & Editing, Formal analysis **Radka Simerova**: Resources, **Petr Sezemsky**: Resources, **Vitezslav Stranak**: Resources, **Mateusz Śmietana**: Resources, Writing - Review & Editing, **Ignacio R. Matias**: Supervision, Writing - Review & Editing.

Declaration of Competing Interest

The authors declare that they have no known competing financial interests or personal relationships that could have appeared to influence the work reported in this paper.

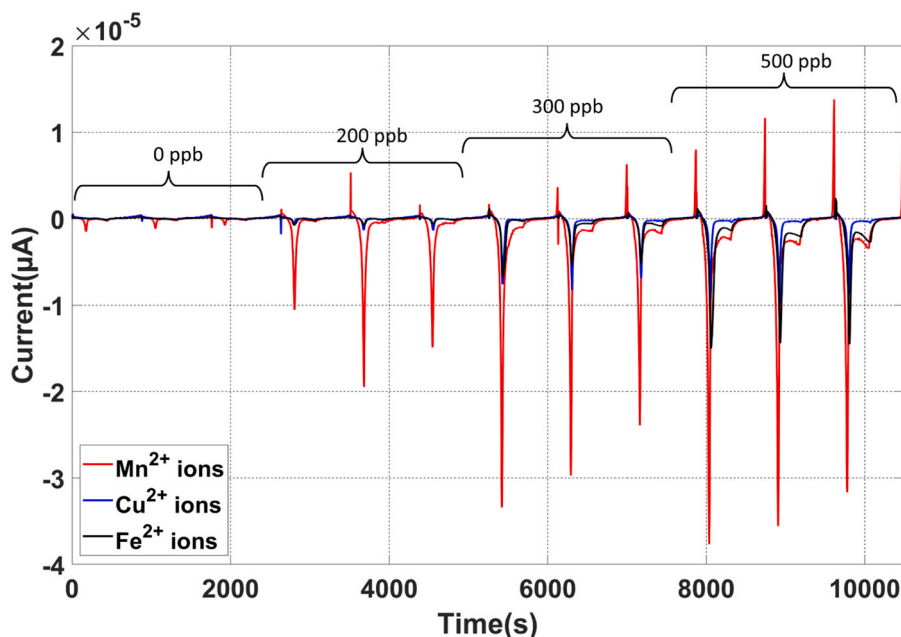**Data availability**

Data will be made available on request.

Fig. 9. Current sensorgrams of the selectivity experiments carried out with Mn^{2+}, Fe^{2+} and Cu^{2+} ions.

Acknowledgments

Appendix A. Supporting information

Supplementary data associated with this article can be found in the online version at doi:10.1016/j.snb.2023.134446.

References

[1] K.M. Andruska, B.A. Racette, Neuromythology of manganism, Curr. Epidemiol. Rep. 2 (2015) 143–148, https://doi.org/10.1007/s40471-015-0040-x.

[2] European Parliament and of the Council, Directive (EU) 2020/2184 of the European Parliament and of the Council of December 16, 2020 on the quality of water intended for human consumption, Official Journal of the European Union. 2019 (2020) 1–62. ⟨https://www.boe.es/doue/2020/435/L00001–00062.pdf⟩.

[3] Agency for Toxic Substances and Disease Registry (ATSDR, Toxicological profile for manganese, atlanta: United States department of health and human services, Agency Toxic. Subst. Dis. Regist. (2012), https://doi.org/10.1201/9781420061888_ch4.

[4] M. Golasik, M. Herman, W. Piekoszewski, E. Gomółka, G. Wodowski, S. Walas, Trace determination of manganese in urine by graphite furnace atomic absorption spectrometry and inductively coupled plasma-mass spectrometry, Anal. Lett. 47 (2014) 1921–1930, https://doi.org/10.1080/00032719.2014.888729.

[5] C.S. Chin, A., K.S. Johnson, K.H. Coale, Spectrophotometric determination of dissolved manganese in natural waters with 1-(2-pyridylazo)-2-naphthol: application to analysis in situ in hydrothermal plumes, Mar. Chem. 37 (1992) 65–82, https://doi.org/10.1016/0304-4203(92)90057-H.

[6] C. Bhatia, S.H. Byun, D.R. Chettle, M.J. Inskip, W. v Prestwich, A neutron activation technique for manganese measurements in humans, J. Trace Elem. Med. Biol. 31 (2015) 204–208, https://doi.org/10.1016/j.jtemb.2014.07.018.

[7] T. Dučić, E. Barski, M. Salome, J.C. Koch, M. Bähr, P. Lingor, X-ray fluorescence analysis of iron and manganese distribution in primary dopaminergic neurons, J. Neurochem 124 (2013) 250–261, https://doi.org/10.1111/jnc.12073.

[8] X. Pei, W. Kang, W. Yue, A. Bange, W.R. Heineman, I. Papautsky, Disposable copper-based electrochemical sensor for anodic stripping voltammetry, Anal. Chem. 86 (2014) 4893–4900, https://doi.org/10.1021/ac500277j.

[9] R.D. Crapnell, C.E. Banks, Electroanalytical overview: The determination of manganese, Sens. Actuators Rep. 4 (2022), 100110, https://doi.org/10.1016/j.snr.2022.100110.

[10] J.S. Roitz, K.W. Bruland, Determination of dissolved manganese(II) in coastal and estuarine waters by differential pulse cathodic stripping voltammetry, Anal. Chim. Acta 344 (1997) 175–180, https://doi.org/10.1016/S0003-2670(97)00041-X.

[11] A.J. Saterlay, J.S. Foord, R.G. Compton, Sono-cathodic stripping voltammetry of manganese at a polished boron-doped diamond electrode: Application to the determination of manganese in instant tea, Analyst 124 (1999) 1791–1796, https://doi.org/10.1039/a906851a.

[12] W. Yue, A. Bange, B.L. Riehl, B.D. Riehl, J.M. Johnson, I. Papautsky, W. R. Heineman, Manganese detection with a metal catalyst free carbon nanotube electrode: anodic versus cathodic stripping voltammetry, Electroanalysis 24 (2012) 1909–1914, https://doi.org/10.1002/elan.201200302.

[13] W. Kang, X. Pei, A. Bange, E.N. Haynes, W.R. Heineman, I. Papautsky, Copper-based electrochemical sensor with palladium electrode for cathodic stripping voltammetry of manganese, Anal. Chem. 86 (2014) 12070–12077, https://doi.org/10.1021/ac502882s.

[14] W. Kang, C. Rusinek, A. Bange, E. Haynes, W.R. Heineman, I. Papautsky, Determination of manganese by cathodic stripping voltammetry on a microfabricated platinum thin–film electrode, Electroanalysis 29 (2017) 686–695, https://doi.org/10.1002/elan.201600679.

[15] I. Zudans, J.R. Paddock, H. Kuramitz, A.T. Maghasi, C.M. Wansapura, S.D. Conklin, N. Kaval, T. Shtoyko, D.J. Monk, S.A. Bryan, T.L. Hubler, J.N. Richardson, C. J. Seliskar, W.R. Heineman, Electrochemical and optical evaluation of noble metal- and carbon-ITO hybrid optically transparent electrodes, J. Electroanal. Chem. 565 (2004) 311–320, https://doi.org/10.1016/j.jelechem.2003.10.025.

[16] J.N. Richardson, A.L. Dyer, M.L. Stegemiller, I. Zudans, C.J. Seliskar, W. R. Heineman, Spectroelectrochemical sensing based on multimode selectivity simultaneously achievable in a single device. 13. Detection of aqueous iron by in situ complexation with 2,2′-bipyridine, Anal. Chem. 74 (2002) 3330–3335, https://doi.org/10.1021/ac0111715.

[17] N. Kaval, C.J. Seliskar, W.R. Heineman, Spectroelectrochemical sensing based on multimode selectivity simultaneously achievable in a single device. 16. Sensing by fluorescence, Anal. Chem. 75 (2003) 6334–6340, https://doi.org/10.1021/ac0347664.

[18] S.E. Andria, C.J. Sellskar, W.R. Heineman, Simultaneous detection of two analytes using a spectroelectrochemical sensor, Anal. Chem. 82 (2010) 1720–1726, https://doi.org/10.1021/ac902243u.

[19] Y. Shi, C.J. Seliskar, W.R. Heineman, Spectroelectrochemical sensing based on multimode selectivity simultaneously achievable in a single device. 2. Demonstration of selectivity in the presence of direct interferences, Chem. Instrum.: A Syst. Approach 66 (1994) 2. ⟨https://pubs.acs.org/sharingguidelines⟩.

[20] J.M. DiVirgilio-Thomas, W.R. Heineman, C.J. Seliskar, Spectroelectrochemical sensing based on multimode selectivity simultaneously achievable in a single device. 6. Sensing with a mediator, Anal. Chem. 72 (2000) 3461–3467, https://doi.org/10.1021/ac991418m.

[21] J.D. Benck, B.A. Pinaud, Y. Gorlin, T.F. Jaramillo, Substrate selection for fundamental studies of electrocatalysts and photoelectrodes: Inert potential

windows in acidic, neutral, and basic electrolyte, PLoS One 9 (2014), e107942, https://doi.org/10.1371/journal.pone.0107942.

[22] C.A. Rusinek, A. Bange, M. Warren, W. Kang, K. Nahan, I. Papautsky, W. R. Heineman, Bare and polymer-coated indium tin oxide as working electrodes for manganese cathodic stripping voltammetry, Anal. Chem. 88 (2016) 4221–4228, https://doi.org/10.1021/acs.analchem.5b03381.

[23] C.A. Rusinek, W. Kang, K. Nahan, M. Hawkins, C. Quartermaine, A. Stastny, A. Bange, I. Papautsky, W.R. Heineman, Determination of manganese in whole blood by cathodic stripping voltammetry with indium tin oxide, Electroanalysis 29 (2017) 1850–1853, https://doi.org/10.1002/elan.201700137.

[24] I. del Villar, C.R. Zamarreño, M. Hernaez, F.J. Arregui, I.R. Matias, Lossy mode resonance generation with indium-tin-oxide-coated optical fibers for sensing applications, J. Light. Technol. 28 (2010) 111–117, https://doi.org/10.1109/JLT.2009.2036580.

[25] I. del Villar, C.R. Zamarreño, M. Hernaez, F.J. Arregui, I.R. Matias, Resonances in coated long period fiber gratings and cladding removed multimode optical fibers: a comparative study, Opt. Express 18 (2010) 20183, https://doi.org/10.1364/oe.18.020183.

[26] I. Del Villar, F.J. Arregui, C.R. Zamarreño, J.M. Corres, C. Bariain, J. Goicoechea, C. Elosua, M. Hernaez, P.J. Rivero, A.B. Socorro, A. Urrutia, P. Sanchez, P. Zubiate, D. Lopez, N. De Acha, J. Ascorbe, I.R. Matias, Optical sensors based on lossy-mode resonances, Sens Actuators B Chem. 240 (2017) 174–185, https://doi.org/10.1016/j.snb.2016.08.126.

[27] M. Śmietana, M. Koba, P. Sezemsky, K. Szot-Karpińska, D. Burnat, V. Stranak, J. Niedziółka-Jönsson, R. Bogdanowicz, Simultaneous optical and electrochemical label-free biosensing with ITO-coated lossy-mode resonance sensor, Biosens. Bioelectron. 154 (2020), 112050, https://doi.org/10.1016/j.bios.2020.112050.

[28] P. Sezemsky, D. Burnat, J. Kratochvil, H. Wulff, A. Kruth, K. Lechowicz, M. Janik, R. Bogdanowicz, M. Cada, Z. Hubicka, P. Niedziałkowski, W. Białobrzeska, V. Stranak, M. Śmietana, Tailoring properties of indium tin oxide thin films for their work in both electrochemical and optical label-free sensing systems, Sens Actuators B Chem. 343 (2021), https://doi.org/10.1016/j.snb.2021.130173.

[29] M. Smietana, B. Janaszek, K. Lechowicz, P. Sezemsky, M. Koba, D. Burnat, M. Kieliszczyk, V. Stranak, P. Szczepański, Electro-optically modulated lossy-mode resonance, Nanophotonics 11 (2022) 593–602, https://doi.org/10.1515/nanoph-2021-0687.

[30] W. Kaim, J. Fiedler, Spectroelectrochemistry: The best of two worlds, Chem. Soc. Rev. 38 (2009) 3373–3382, https://doi.org/10.1039/b504286k.

[31] M. Śmietana, M. Sobaszek, B. Michalak, P. Niedziałkowski, W. Białobrzeska, M. Koba, P. Sezemsky, V. Stranak, J. Karczewski, T. Ossowski, R. Bogdanowicz, Optical monitoring of electrochemical processes with ITO-based lossy-mode resonance optical fiber sensor applied as an electrode, J. Light. Technol. 36 (2018) 954–960, https://doi.org/10.1109/JLT.2018.2797083.

[32] T. Okazaki, M. Yoshioka, T. Orii, A. Taguchi, H. Kuramitz, T. Watanabe, Electrochemical lossy mode resonance-based fiber optic sensing for electroactive species, Electroanalysis 34 (2022) 1–9, https://doi.org/10.1002/elan.202200089.

[33] M. Koba, D. Burnat, K. Szot-Karpińska, P. Sezemsky, V. Stranak, R. Bogdanowicz, J. Niedziółka-Jönsson, M. Śmietana, Combined optical and electrochemical analysis of protein binding with ITO-coated lossy-mode resonance sensor, in: Seventh European Workshop on Optical Fibre Sensors (EWOFS 2019), 2019: p. 96. https://doi.org/10.1117/12.2540849.

[34] M. Sobaszek, D. Burnat, P. Sezemsky, V. Stranak, R. Bogdanowicz, M. Koba, K. Siuzdak, M. Śmietana, Enhancing electrochemical properties of an ITO-coated lossy-mode resonance optical fiber sensor by electrodeposition of PEDOT:PSS, Opt. Mater. Express 9 (2019) 3069, https://doi.org/10.1364/ome.9.003069.

[35] R. Bogdanowicz, P. Niedziałkowski, M. Sobaszek, D. Burnat, W. Białobrzeska, Z. Cebula, P. Sezemsky, M. Koba, V. Stranak, T. Ossowski, M. Śmietana, Optical detection of ketoprofen by its electropolymerization on an indium tin oxide-coated optical fiber probe, Sensors 18 (2018) 1–15, https://doi.org/10.3390/s18051361.

[36] P. Niedziałkowski, W. Białobrzeska, D. Burnat, P. Sezemsky, V. Stranak, H. Wulff, T. Ossowski, R. Bogdanowicz, M. Koba, M. Śmietana, Electrochemical performance of indium-tin-oxide-coated lossy-mode resonance optical fiber sensor, Sens Actuators B Chem. 301 (2019), 127043, https://doi.org/10.1016/j.snb.2019.127043.

[37] A. Azlan, H.E. Khoo, M.A. Idris, A. Ismail, M.R. Razman, Evaluation of minerals content of drinking water in malaysia, Sci. World J. 2012 (2012), https://doi.org/10.1100/2012/403574.

[38] AOAC INTERNATIONAL, Appendix F: Guidelines for Standard Method Performance Requirements, 2016. https://www.aoac.org/resources/guidelines-for-standard-method-performance-requirements/ (accessed June 4, 2023).

[39] Ismel Dominguez, Jesus Corres, R. Ignacio, Matias Joaquín Ascorbe, Ignacio del Villar, High sensitivity Lossy-Mode Resonance refractometer using low refractive

index PFA planar waveguide, Opt. Laser Technol. 162 (2023), https://doi.org/10.1016/j.optlastec.2023.109235.

[40] I. Dominguez, I. Del Villar, O. Fuentes, J.M. Corres, I.R. Matias, Dually nanocoated planar waveguides towards multi-parameter sensing, Sci. Rep. 11 (2021), 3669, https://doi.org/10.1038/s41598-021-83324-8.

Ismel Domínguez received the degree in telecommunications and electronics engineering from the University "Hermanos Saiz Montes de Oca" (UPR), Pinar del Rio, Cuba, in 2009. He is currently pursuing the Ph.D. degree with the Department of Electrical and Electronic Engineering, Public University of Navarra (UPNA). His current research focuses on optical fiber sensors, microfluidics, and spectroelectrochemistry systems.

Jesus M. Corres received the MS degree in electrical engineering from the Public University of Navarra, Pamplona, Spain, in 1996 and the PhD degree from the Public University of Navarra, Pamplona, Spain in 2003. Currently he works as Full Professor in the Department of Electrical and Electronic Engineering (UPNA). His main research is the development of fiber optic sensors using nanostructured materials for biomedical, environmental and safety applications. He is the author or co-author of more than 100 publications and serves as associate editor of IEEE Sensor Letters

Ignacio del Villar received his MS degree in Electrical and Electronic Engineering and his Ph.D. degree, specialty in Optical Fiber Sensors, in 2002 and 2006, respectively, from the Public University of Navarra (UPNA). Since 2021, he has been an Associate Professor with the Public University of Navarra. He has coauthored more than 200 chapter books, journals and conference papers in his research areas, which include optical fiber sensors and the effect of nanostructured coatings deposited on waveguides. He is also the Co-Founder of two spin-off companies: Eversens and Pyroistech

Juan D. Mozo received his B.Sc. and Ph.D. degrees in chemistry from the University of Seville in 1991 and 1997 respectively. Currently, he is Associate Professor of Physical Chemistry at the University of Huelva. He has specialized in electrochemistry area and his research is mainly focused on the development of laboratory instrumentation for (flow) electroanalytical techniques and spectroelectrochemical measurements.

Radka Simerova is a junior researcher and currently a student at University of South Bohemia. She is interested in plasma assisted deposition of thin functional films, namely those employed as transducer or sensors structures. Besides she carries electrochemical measurements, thin film analyzes and diagnostics of plasma.

Petr Sezemsky is a Ph.D. student at the University of South Bohemia in branch of Biophysics. His work is focused on research and deposition of bioactive and biofunctional surfaces. His field of interest is low-temperature plasma deposition, bio-functional and antibacterial surfaces, sensor technique.

Vitezslav Stranak received a Ph.D. from the Charles University in Prague, Czech Republic in 2007. Afterwards he was a postdoctoral fellow in Greifswald (Germany) oriented on low-temperature plasma diagnostics and deposition of thin film. Since 2013 he is with University of South Bohemia, Czech Republic as associated professor performing applied research of thin nanostructured and functional thin films.

Mateusz Śmietana received his B.Sc., M.Sc., Ph.D. (with distinction), and D.Sc. degrees in electronics from the Warsaw University of Technology (WUT), Poland, in 2000, 2002, 2007, and 2014, respectively. Since December 2015 he has been an Associate Professor in the Institute of Microelectronics and Optoelectronics, WUT. He was a postdoctoral fellow at Virginia Tech, USA and Université du Québec en Outaouais, Canada, as well as a visiting professor at Southern University of Science and Technology (China). He has authored and co-authored more than 120 scientific papers. His fields of interest are fiberoptic sensors and thin films.

Ignacio R. Matias received the M.S. degree in Electrical and Electronic Engineering and his Ph.D. degree in Optical Sensors from the Polytechnic University of Madrid (UPM), Madrid, Spain, in 1992 and 1996, respectively. He became a Lecturer at the Public University of Navarra (Pamplona, Spain) in 1998, where he is a Full Professor since 2006. He has co-authored more than 250 journal, 300 conference papers, 2 books and 21 book chapters related to optical sensors and systems and has participated in the founding of 5 spin-offs related to sensors. He was founding Associate Editor of the IEEE Sensor Journal in 2001, Topical Editor from 2012 to 2016, Senior Editor since 2008 and IEEE Fellow for contributions to photonic sensor research and transference to industry since 2023.